An Indoor Airborne Ultrasonic Wireless Communication Network

Wentao Jiang, and William M. D. Wright, *Senior Member, IEEE*

***Abstract*—There is an increasing interest in the use of modulated airborne ultrasound as a means of indoor wireless communication. By using commercially available capacitive ultrasonic transducers at 50 kHz, this paper describes the successful practical implementation of a prototype airborne ultrasonic communication network with ceiling-mounted base stations and a mobile transceiver unit. An asynchronous ultrasonic location technique using Gold code modulated ranging signals was chosen to optimise the modulation schemes and data transfer, and offered automatic handover between different cell regions on a switch on and off basis as all base stations used the same frequency bands for data transmission. 16-quadrature amplitude modulation (QAM) based on orthogonal frequency division multiplexing (OFDM) was used to achieve an uplink data transfer rate of 37.4 kb/s while the range was extended by using quadrature phase-shift keying (QPSK)-OFDM with a data rate of 18.7 kb/s. For the uplink connection, the achieved data rates using 16QAM-OFDM and QPSK-OFDM were 36.1 kb/s and 18.1 kb/s, respectively. A more robust handover technique using received signal strength with hysteresis was also proposed to improve system efficiency when multiple mobile receivers used the service.**

Keywords*— *airborne ultrasonic communication; handover schemes; orthogonal frequency division multiplexing (OFDM); ultrasonic positioning

I. Introduction

Communication systems using modulated ultrasound have been developed previously for underwater applications [1]–[4]. As ultrasound generation, propagation and detection in air is more difficult, more susceptible to changes in atmospheric conditions and attenuation is significant [5], most airborne ultrasonic communication systems to date have been investigated for indoor use only [6]–[10].

Due to the increasing demands of ubiquitous connectivity, the radio frequency (RF) spectrum resource is becoming crowded, and interference between neighbouring systems is inevitable [11], [12]. Therefore, using ultrasound in air could be a good short-range low-data-rate alternative to RF connections. Moreover, if secure data transmission links are required, indoor airborne ultrasonic systems can provide a higher level of privacy since ultrasound does not penetrate through most solid barriers which makes interception or hacking from outside the building very difficult. Potential applications could be personal guide systems for providing highly localised information or more secure access to individual localised peripheral devices in an open office environment.

Previously reported ultrasonic indoor networks were used primarily for indoor positioning [13]–[15]. This paper will describe the implementation of a prototype indoor ultrasonic communication network with full-duplex connections. The next section will introduce the characterization of the ultrasonic transducers used for this work. Section III discusses the architecture planning of the communication network based on experimental results. To enable the system to switch between different modulation schemes for more efficient and reliable signal transmission, the user location must be determined. Section IV gives a brief review of ultrasonic positioning systems in the literature, followed by a description of the positioning method used, the generation of the ranging signal, and the evaluation of the location accuracy. After that, the handover scheme for a system with a moving transceiver unit (one transmitter and one receiver) will be introduced. The last section gives the conclusions of this work.

This work was supported by Science Foundation Ireland (SFI) Research Frontiers Programme grant number 11/RFP.1/ECE3119.

II. Ultrasonic transducer characterization

The ultrasonic transducers used in this work were commercially available SensComp series 600 environmental grade transducers [16]. These transducers had a measured 6-dB bandwidth of about 22 kHz from 44 to 65 kHz as shown in Fig. 1 (a), using the same experimental setup as described previously in [10]. More recently obtained SensComp transducers had a more concentrated frequency response at the nominal frequency of 50 kHz than the SensComp devices used previously in [10]. The measured signal-to-noise ratio (SNR) value was 38.3 dB over a range of 2 m. The system phase response is shown in Fig. 1 (b), indicating zero phase distortion across the ultrasonic bands from 20 kHz to 150 kHz.

The experiment was initially conducted using 16-quadrature amplitude modulation (QAM) based on an orthogonal frequency division multiplexing (OFDM) scheme [10] over frequencies from 30 kHz to 79 kHz. The symbol time was set at 1 ms, so that there were 50 subchannel signals with an overall data rate of 200 kb/s being transmitted through the air gap. The decoding bit errors of the received signal at a SNR level of 29.6 dB over 5 m were calculated as the error distribution at different subcarriers is shown in Fig. 2. As can be seen, the error distribution presents a U-shape pattern corresponding to the shape of the system frequency response curve in Fig. 1(a). More bit errors occurred in less responsive subchannels. According to the bit error rate result in Fig. 2, subchannels from 45 kHz to 65 kHz with the minimum number of decoding errors were used to transmit 16-QAM modulated signals at 80 kb/s in both simplex and full-duplex configurations. The resulting received signal constellation diagrams are shown in Fig. 3 (a) and (b), respectively. As can be seen, in simplex mode, all decoded sub-carrier signal constellations are clustered around the target points with no measurable errors, while the received constellations

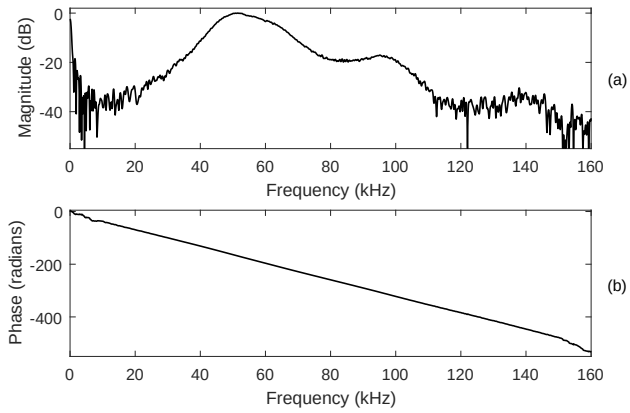

Fig. 1: System characteristics over 2 m: (a) frequency response; and (b) phase response.

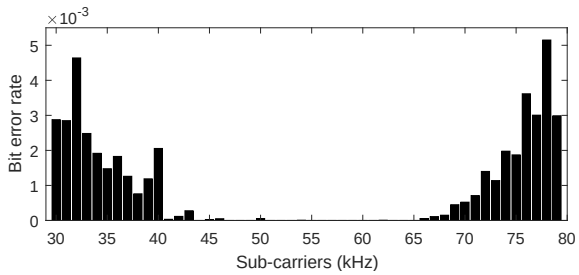

Fig. 2: Error distribution at different sub-carriers from 30 kHz to 79 kHz over 5 m.

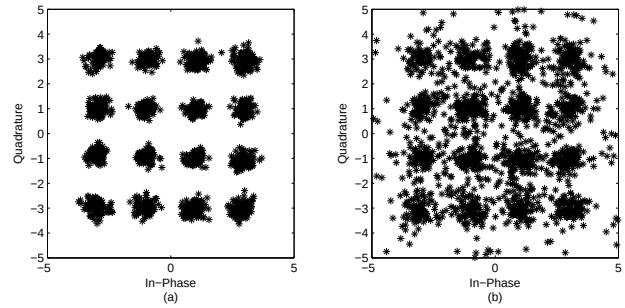

Fig. 3: Received signal constellation at 5 m in (a) simplex, and (b) full-duplex mode.

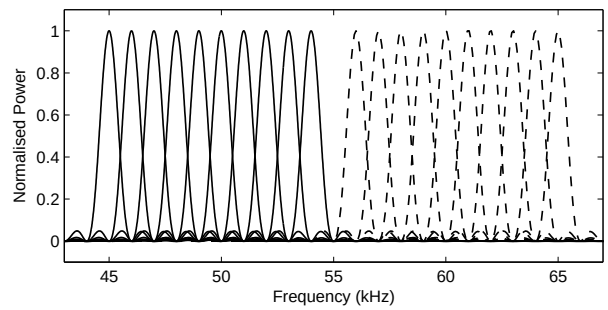

Fig. 4: Outward (solid line) and return (dashed line) signal spectra at separate bands.

are dispersed across the detection boundaries in full-duplex mode. This is due to the interference between the two signals contra-propagating simultaneously across the air gap in the same frequency channels. By splitting the frequency bands for signals transmitting in opposite directions, this interference can be eliminated. The theoretical spectra for both outward and return OFDM modulated signals are shown in Fig. 4. As can be seen, distinctive peaks can be found at all orthogonal sub-carriers, and they are divided into two groups with a 1-kHz guard band at 55 kHz. In this case, the data rate was reduced to 40 kb/s for the transmission in each direction.

III. Network architecture

A basic indoor communication network structure has ceiling-mounted or wall-mounted base stations with fixed transceivers and one or more mobile transceivers within the network area. The ultrasonic beam emitted by a flat circular transducer aperture can be considered as a cone due to diffraction and beam spreading, therefore the projection at any normal distance away from the aperture is a circle with a radius which depends on the range and the transmitted signal frequency. Therefore, any network configuration will be a compromise between coverage and data rate. Over short ranges, a higher data rate can be achieved with a small coverage area, however, requiring a higher number of transceivers. Over long ranges, the achieved data rate might be lower with relatively large signal coverage, but a smaller number of transceivers is needed. Thus, a reasonable compromise between the two is required.

One popular network architecture divides the geographic service area into hexagonal zones, as employed in cellular mobile communication systems [17]. A cell is the volume serviced by one base station with one transceiver. Fig. 5 shows a typical cell plan using hexagonal divisions of the same size, and the coverage region overlaps at the outer boundaries. Since a hexagonal cell has an equal distance to all adjacent cells, it provides the most efficient coverage. The corresponding side view of the base station and mobile unit setup is shown in Fig. 6. As can be seen, the base stations are placed on the ceiling with their transceivers facing down to the ground. The mobile transceiver is placed under the coverage area facing the ceiling. As the highest frequency channel used for data transmission is 65 kHz using separate bands for uplink and downlink as described in Section II, the maximum possible theoretical angle of divergence at this frequency is $9.65°$, giving a coverage circle with a radius of 0.47 m when the height of the base stations relative to the height of the mobile unit is fixed at 2.75 m. Therefore, the maximum separation between the two base stations should be less than 0.94 m. If the height of the mobile device is higher than 0.46 m, there are ”blind zones” between the beams of different base stations. This system is just a first prototype to demonstrate proof of concept, so transducers with a wider beam divergence angle are recommended for future systems.

To maximise the system throughput, data transmissions were carried out using 16QAM-OFDM modulation at different lateral displacements in full-duplex mode. The maximum error-free lateral displacement was 0.2 m for both uplink and downlink with separated bands. By using quadrature phase-

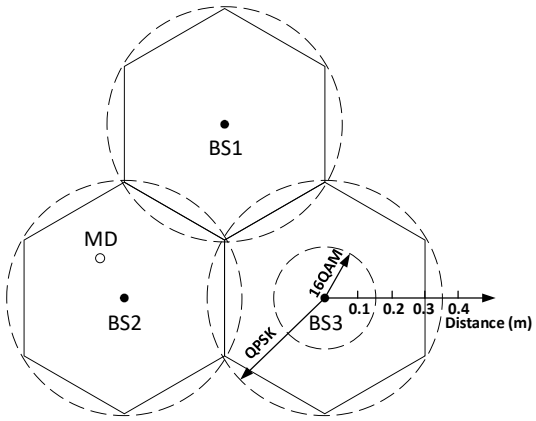

Fig. 5: Cell planning using hexagonal shapes. The solid lines indicate the boundaries of cells, the dashed lines indicate the signal coverage region, BS (●) represents base stations, and MD (○) represents the mobile device.

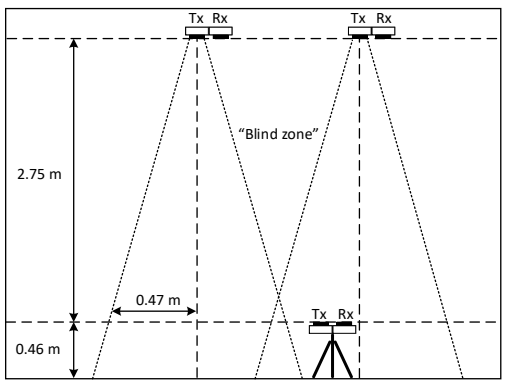

Fig. 6: Side view of the indoor network setup including ceiling-mounted base stations and a mobile transceiver unit with their transmitting beam contours indicated.

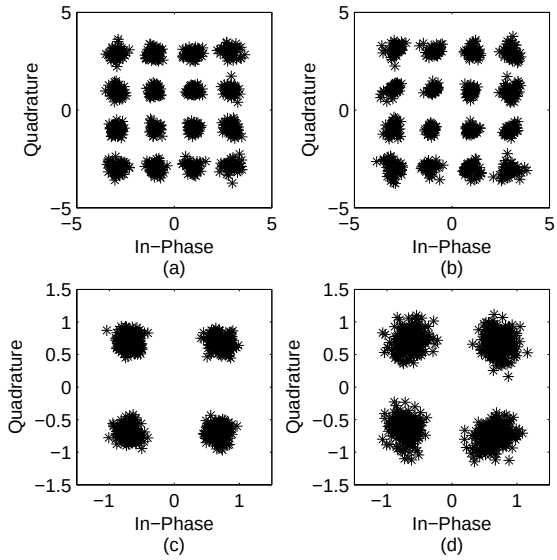

Fig. 7: The received 16QAM-OFDM uplink (a) and downlink (b) signal constellation at a lateral displacement of 0.15 m; and QPSK-OFDM uplink (c) and downlink (d) signal constellation at a lateral displacement of 0.35 m in full-duplex mode.

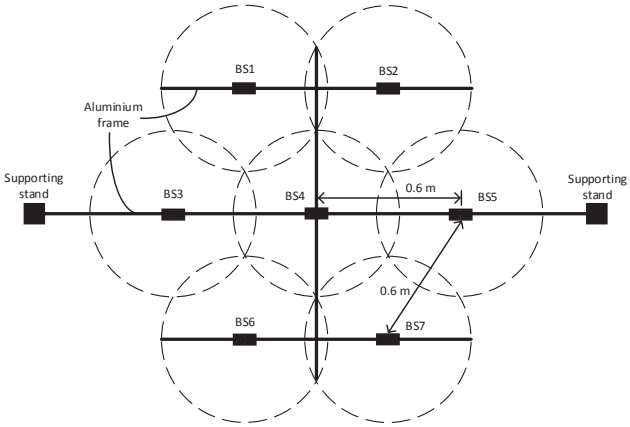

Fig. 8: Schematic of the base stations installed on the ceiling.

shift keying (QPSK)-OFDM, the maximum lateral displacements with no measurable errors were extended up to 0.45 m and 0.4 m for uplink and downlink, respectively. These could be identically sized using interleaved uplink and downlink channels, but at the expense of the maximum data rate achievable. The received 16QAM-OFDM signal constellations for the uplink and downlink at a lateral displacement of 0.15 m were shown in Fig. 7 (a) and (b), respectively. Similarly, the received QPSK-OFDM signal constellations for the uplink and downlink at a lateral displacement of 0.35 m were also shown in Fig. 7 (c) and (d). Both the downlink constellations using different modulations show larger variations in phase and amplitude than that of the uplink signals. This is because by using lower frequency bands the uplink signal has a wider angle of divergence for better signal reception at the same lateral displacement compared to the downlink signal. Therefore, to maintain a reliable full-duplex data transmission link, at least two different modulation methods should be used at different coverage regions as shown in Fig. 5. In this case, 16QAM-OFDM can provide a maximum data transfer rate of 40 kb/s for both uplink and downlink within a circle radius of 0.15 m. For a larger reliable coverage area, the radius can be extended up to 0.35 m using QPSK-OFDM at a reduced data rate of 20 kb/s for both uplink and downlink. A larger error-free region may achieved by using lower order modulation, binary phase-shift keying (BPSK)-OFDM, but it was not used in this work due to its low transfer rate of 10 kb/s. The horizontal separation of two different cell centres was set at 0.6 m to achieve seamless and reliable connectivity between the mobile transceiver and the base stations. The ceiling mounted base station network is illustrated in Fig. 8. Each base station had one transmitter and one receiver that were attached to an aluminium frame. All transducers could have their positions adjusted on the metal frame as shown in Fig. 9. To show proof of principle, seven pairs of ultrasonic transducers covered an area of about 2.2 m^2.

As the SensComp ultrasonic sensors had a nominal frequency of 50 kHz, only limited bandwidth could be used

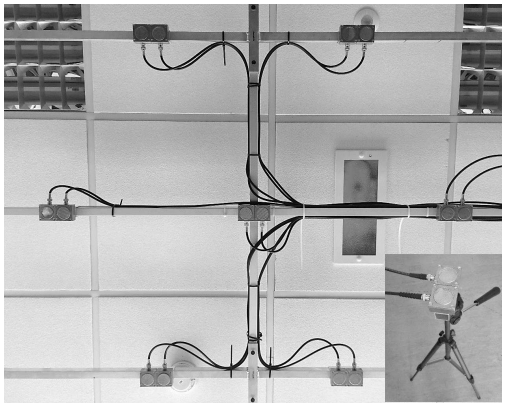

Fig. 9: Installed ceiling-mounted base stations and the mobile transceiver overlaid on the right bottom corner.

for data transmission. In addition, the emitted sound beam was highly directional due to the relatively small value of λ/D (ratio of signal wavelength and transducer diameter). It reduced the effective horizontal coverage area, and affected the accuracy of the data exchange with large lateral displacement. Therefore, broadband ultrasonic transducers with a wide divergent angle design would be preferable for a more effective indoor communication system. Recent work using 3D-printed waveguides and beam steering [18] could also be used.

IV. Ultrasonic Positioning

For an indoor ultrasonic communication network, the knowledge of user location is important for selection and optimization of the modulation scheme. Due to the low propagation speed of ultrasound in air compared with radio waves, ultrasonic systems can provide more accurate measurement of time-of-flight (TOF) for location estimation.

A number of ultrasonic indoor positioning and localization systems have been reported in the literature. The Bat system [13] consisted of mobile wireless devices and a network of fixed ceiling-mounted receivers. By emitting a radio-triggered ultrasonic pulse from the users, the system measured the TOFs of the pulse intercepted by different receivers and calculated the 3D position of the mobile device by triangulation. The achieved positioning accuracy was within 3 cm at 40 kHz. The Cricket system [19] allowed mobile and static nodes to learn their physical locations by receiving and analysing concurrent radio and ultrasonic signals at 40 kHz from beacons spread throughout the building, achieving a 3D position accuracy between 5 cm and 25 cm [20]. Another similar indoor position sensing system [21] allowed wearable and mobile computers to determine their positions in a 3D space by receiving precisely timed 40 kHz ultrasonic signals triggered by a RF pulse from four transmitters installed on the ceiling using TOF methods. The resulting positioning accuracy was between 10 cm and 25 cm. A later study has looked at an indoor positioning system using prototype Dolphin transmitters and receivers at 50 kHz without radio triggering [8]. This centralised system with ceiling receivers and roaming transmitters was shown to have 2 cm location accuracy. In [22], a reference-free ultrasonic indoor location system with a receive-only mobile device which determined its own position based on ultrasonic signals in frequency bands between 36 kHz and 45 kHz sent by at least three transmit-only ultrasonic beacons was proposed. The mobile device consisted of three receivers placed in a triangle, allowing angle-of-arrival and TOF estimation without the use of synchronising RF. The system provided 3D location accuracy of about 9.5 cm. Recent work has implemented an ultrasonic local positioning system that allowed a mobile robot to navigate in an indoor area [23]. Each ceiling-mounted beacon contained five ultrasonic transducers which sent positioning signals modulated using orthogonal codes at 40 kHz. The ultrasonic signals were synchronised by RF pulses, and the achieved position accuracy was below 3 cm.

A. Positioning method

It is common to use the slow propagation speed of ultrasound to estimate its TOF between a transmitter and a receiver. The TOF is then used to calculate the distance between the two nodes based on the measured speed of sound in air. A receiver collects a set of transmitter-to-receiver distances to estimate its position by using the mathematical method of trilateration. A roaming receiver's 3D position (R_x, R_y, R_z) is a function of the measured distance d_i to a given ceiling transmitter i, and the preassigned location (x_i, y_i, z_i) of the fixed beacon transmitter, described as

$$d_i = \sqrt{(R_x - x_i)^2 + (R_y - y_i)^2 + (R_z - z_i)^2}. \quad (1)$$

In order to perform trilateration, at least three different values of d_i are required. In addition, the receiver needs to know the exact time that the ranging signals depart from the transmitters to calculate the absolute TOFs. Therefore, a wireless RF synchronization signal is often sent synchronously to achieve good accuracy [13], [19], [21]. However, the inclusion of this synchronization link to provide a timing reference may increase the hardware complexity and requires the use of RF which may not be desirable.

There is another TOF method, in which the mobile receiver only measures the time differences of the arriving ultrasonic signals with respect to each other rather than the absolute TOFs. Therefore, a set of pseudo-ranges may be gathered with an equal offset from the true transmitter-to-receiver distances [24]. This approach is also performed by Global Positioning System (GPS) receivers using RF satellite signals [25]. The relationship can be expressed as

$$\tilde{d}_i = \sqrt{(R_x - x_i)^2 + (R_y - y_i)^2 + (R_z - z_i)^2} + \Delta d, \quad (2)$$

where $\tilde{d}_i$ is the pseudo-range to a certain transmitter and Δd is the distance offset common to all pseudo-ranges. To perform trilateration, at least four pseudo-ranges are required as there are four unknowns in (2). These asynchronous ultrasonic receivers do not need additional wireless radio-triggered synchronization links to perform position estimation, therefore, simplifying the hardware of the system. However, it takes one more signal TOF measurement to compute the location, making the estimation potentially less accurate.

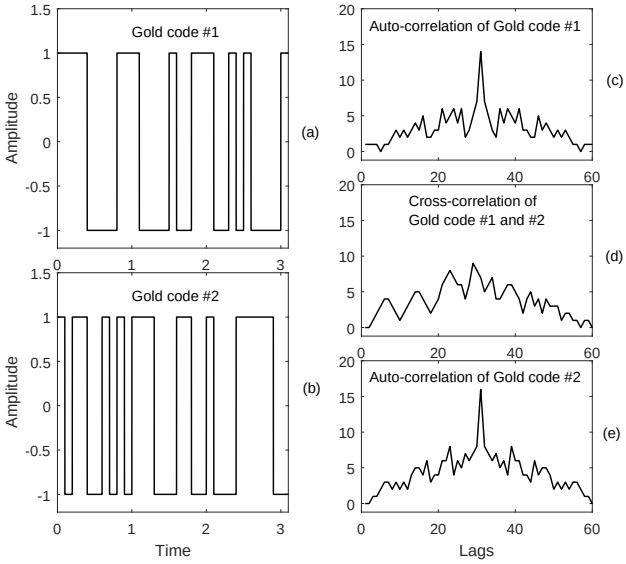

Fig. 10: Gold code and its correlation properties.

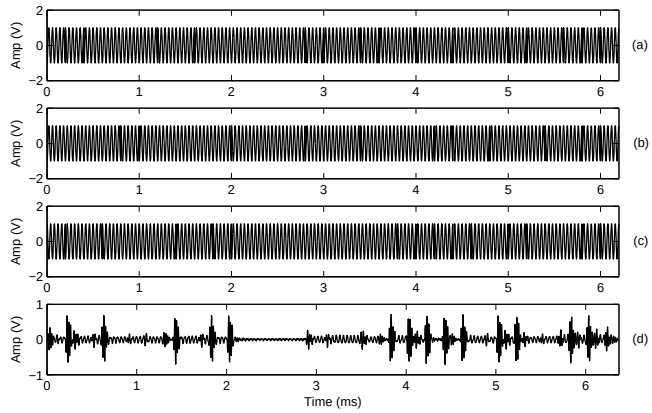

Fig. 11: Transmitted signals (a), (b), (c), carrying Gold codes from three different ceiling-mounted transmitters and the received signal (d) by the mobile device.

B. Ranging signal

Multiple ceiling beacons should transmit their unique ranging signals simultaneously at the same frequency to have the same coverage area and similar received signal strength at the receiver. In the system used in this work, a code division multiple access (CDMA) method was used. CDMA is a spread-spectrum technique that transmits the signals at the same time with different spreading code sequences [26]. Code sequences that have good autocorrelation properties are called pseudorandom noise sequences as their autocorrelation function is similar to that of random noise which has a sharp peak and low sidebands [27].

Gold codes [28] were used in this work as they are a particular set of pseudo-random sequences that are constructed by the XOR of two preferred m-sequences using the same clock signal [29]. As the cell size is relatively small, a fast positioning update rate is needed. Therefore, the length of the m-sequence should be as small as possible. Fig. 10(a) and (b) show two 31-bit Gold sequences from the same family. Their auto-correlations are illustrated in Fig. 10(c) and (e), respectively, indicating high similarities with themselves. Their cross-correlation property is shown in Fig. 10(d), indicating very low correlation with each other. Gold codes are widely used in applications in telecommunication and satellite navigation [30]. Gold codes with a length of 511 bits have also been used previously for indoor location systems using both acoustic [31] and ultrasonic [8] methods.

C. Positioning accuracy evaluation

Location measurements were performed in a laboratory environment using three active ceiling base stations and one mobile transceiver. The base stations were placed near the ceiling in the centre of the room at three adjacent cell positions as shown in Fig. 9, with their apertures facing the floor to minimise the effect of multipath reflections from the walls. The mobile transceiver was placed at different known coordinate points facing the ceiling.

A sinusoid with a low ultrasonic frequency of 25 kHz outside the communication channels (45 to 65 kHz) was used as the carrier wave, modulated by a Gold code using BPSK. The Gold code had a length of 31 bits and was applied at a rate of 5 kHz, yielding a ranging signal duration of 6.2 ms. Each transmitter from the ceiling base stations was assigned a unique Gold code from the same family. The mobile receiver was placed at a fixed height of 0.46 m above the floor to simplify the positioning process. Therefore, as R_z and z_i are now known, (2) simplifies to

$$\tilde{d}_i = \sqrt{(R_x - x_i)^2 + (R_y - y_i)^2 + C} + \Delta d, \qquad (3)$$

where C is a constant equal to $(R_z - z_i)^2$. Fig. 11 (a), (b) and (c) show Gold code modulated ranging signals transmitted simultaneously from three different base stations and received as a single waveform by the mobile device as illustrated in Fig. 11 (d), where the effect of constructive and destructive interference can be seen.

The receiver needs to correlate the received waveform with the different corresponding transmitted Gold code modulated signals. The cross-correlation results of the received signal against the three different ranging signals are shown in Fig. 12 (a), (b) and (c). After peak detection, the highest peaks of the resulting curves illustrated in Fig. 12 (d), (e) and (f) can then be used to identify the TOAs of the ranging signals. It can also be observed that the signal that arrived at the receiver earlier than the others had a higher peak as the transmission distance was shorter thus less attenuation occurred.

The location accuracy of the system was evaluated at ten different positions for the mobile transceiver at a fixed height. The measurements were taken 10 times at each test position. The 2D coordinates of the evaluated test points are shown in Fig. 13. Note that only a coverage area of about 0.5 m^2 is shown here as the transceiver location is determined by any three neighbouring base stations in the network. As can be seen, the measured points are close to the reference points,

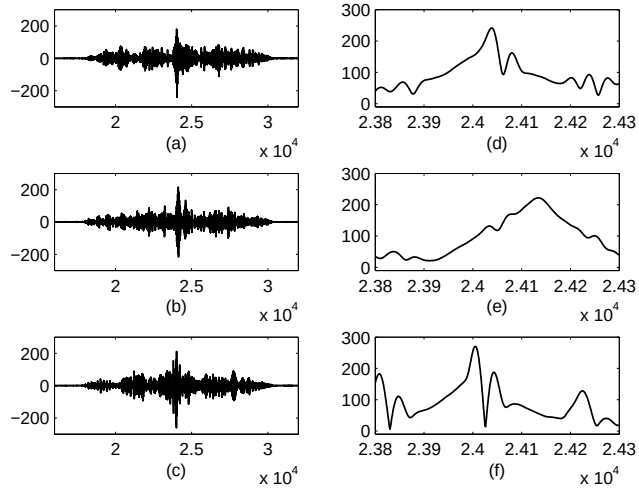

Fig. 12: Cross-correlation of the received ranging signal with different Gold code modulated signals (a), (b), (c), and the resulting curves after peak detection (d), (e), (f).

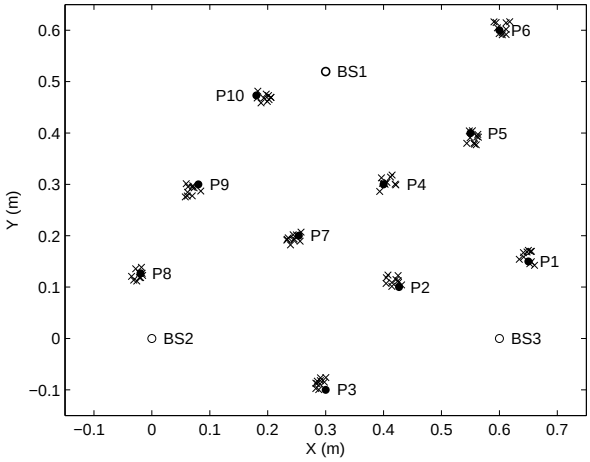

Fig. 13: Estimated 2D positions (x) using asynchronous ranging algorithm in coordinates (X,Y). The solid points (P1-P10) correspond to the positions where the receiver transducer was physically placed, and the unfilled points were the positions of the three ceiling base stations (BS1-BS3).

demonstrating the effectiveness of the positioning system. It should be noted that the signal processing was carried out in MATLAB with a computational effort of about 1.4 s for calculating each position of the mobile device. The signal sampling rate for both generation and acquisition are 1 MHz, resulting a correlation time resolution of 1 µs. Accordingly, the measured locations of base stations and mobile unit had a positional error of ± 1 mm. Fig. 14 shows the cumulative distribution function of the absolute positioning error from the measurements at all ten test points. All the error readings of the estimated locations were within 28.37 mm which is 2.13% of the theoretical radius (1332 mm) that was covered by the cone of the emitted 25 kHz ultrasonic signal sent from the base station. The maximum absolute positioning error was approximately equal to the transducer diameter. It indicates

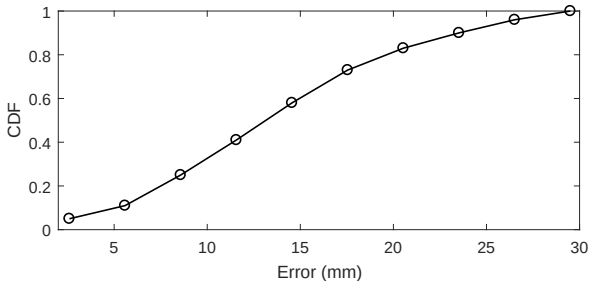

Fig. 14: Cumulative distribution function (CDF) of the absolute positioning error from the measurements carried out at all ten testing points.

that the ultrasonic positioning system using an asynchronous ranging method is feasible with reasonably good accuracy.

V. Handover techniques

In a cellular wireless communication system, a mobile device should be able to move between different cells while still keeping the connection with at least one of the base stations through an automatic and seamless handover [32]. It represents a switching process from one serving base station to a candidate base station. As the mobile unit has a fixed height in this work, the handover allows connectivity switching when the mobile device moves from one active cell to the other horizontally without changing the service network.

With multiple users, base stations in adjacent cells are assigned to different frequencies to prevent co-channel interference. To use the frequency spectrum more efficiently, the corresponding frequencies are re-used in a regular pattern over the entire service area [33]. With a frequency re-use factor of 3, the available frequency spectrum is then divided into three different channel groups for each cluster that contains three adjacent cells. However, the narrowband system used in this work does not have the bandwidth to further split the spectrum into different frequency groups. Therefore, identical uplink and downlink channels were used by all base stations in different cells. The handover process is then to switch off the downlink channels of the current base station, and switch on those of the candidate base station based on the estimated location and trajectory of the mobile transceiver. Note that only one mobile transceiver was used in this system, to show proof of concept, although multiple mobile devices could be supported.

Assuming that the mobile transceiver moves at a constant speed, υ, and the location update rate is η, the minimum detectable distance that the mobile unit has moved is υ/η. As shown in Fig. 5, there is a 50 mm gap between the maximum error-free displacement and the planned cell coverage radius, so the minimum detectable moving distance should then be less than this to ensure reliable switching between different modulation methods within the cell and the handover between adjacent cells. Fig. 15 shows the transmitted signal structure of a base station, using the downlink frequency bands from 56 kHz to 65 kHz. The ranging signal modulated by a Gold code at 25 kHz was sent every 31 ms with a duration of 6.2 ms, thus the achieved system location update rate was

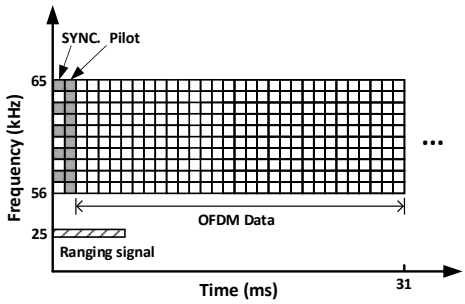

Fig. 15: Signal structure of base stations.

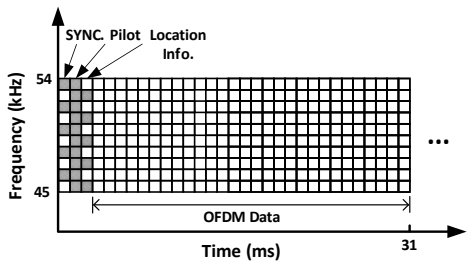

Fig. 16: Signal structure of the mobile device.

32.3 Hz. The value of υ/η was 46.4 mm when the speed of the mobile transceiver was 1.5 m/s. Each signal packet contained a synchronization signal, a pilot signal and 29 OFDM signals carrying data. Therefore, the data rates using 16-QAM and QPSK were 37.4 kb/s and 18.7 kb/s, respectively. For the mobile transceiver, the signal structure as illustrated in Fig. 16 was used, with uplink frequency bands from 45 kHz to 54 kHz. Note that the first packet of the data signals was reserved for sending the calculated location of the mobile transceiver to the base stations so that the system was able to switch between different modulation schemes within the same cell and perform the handover between cells. The achieved uplink data rates using 16-QAM and QPSK were thus 36.1 kb/s and 18.1 kb/s, respectively. Doppler frequency shift due to the movement of the mobile transceiver can shift the subcarriers from their expected frequencies. The measured maximum tolerances with respect to the spacing between two subcarriers were 3% and 12% for 16-QAM and QPSK, respectively. Therefore, to maintain the same data transfer rates without any measurable errors, the maximum horizontal velocity of the mobile transceiver was limited to 2.9 m/s for 16-QAM and 5 m/s for QPSK. However, when the height of the mobile transceiver decreases, the relative horizontal velocity and the effect of Doppler shift reduces accordingly, increasing the robustness of the system.

Ultrasonic transducers with a wider beam divergence would provide a larger signal coverage area. The location update rate could also be reduced to improve the overall data transfer rate as a smaller number of handovers would be needed. When broadband ultrasonic transducers with sufficient transmission bandwidth are used, a frequency re-use scheme could provide services to multiple mobile devices. For example, a cellular system with a frequency re-use factor of 3 would need to share the overall available frequency bands as illustrated in Fig. 17.

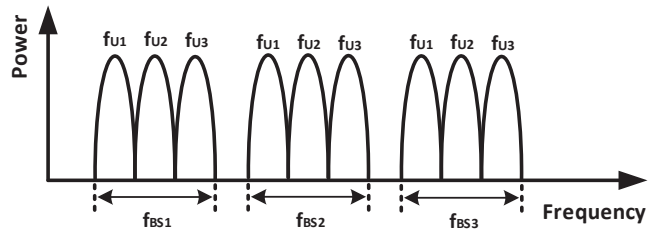

Fig. 17: Channel arrangement for multiple users. f_{U1}, f_{U2} and f_{U3} represent frequency bands for MD1, MD2 and MD3, respectively, and f_{BS1}, f_{BS2} and f_{BS3} represent frequency bands for BS1, BS2 and BS3, respectively.

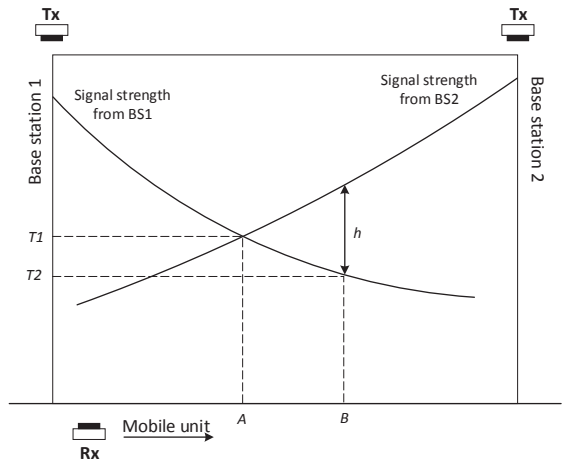

Fig. 18: Handover design for ceiling-mounted network configuration.

Each base station (BS) would need to reserve a dedicated subband (f_{U1}, f_{U2} and f_{U3}) for each of the three mobile devices (MD). An alternative handover technique could use the received signal strength from the current and the adjacent base stations. As Fig. 18 shows, as the mobile device moves from the current base station to an adjacent base station, it keeps detecting the received signals that operate at different frequency bands from both base stations. If the handover occurs at position A when the received signal strengths from two base stations are equal, any fluctuation of the received signal strength may stimulate unnecessary handover attempts when the current base station is still able to provide adequate service. The fluctuation in signals may be introduced by multipath reflections or the orientation of the receiver transducer. When the mobile unit is passing position A and moving towards the adjacent base station (BS2), the received signal strength from the current base station (BS1) may become sufficiently weaker. The handover occurs at position B with a certain amount of hysteresis, h, which could effectively prevent any "ping-pong" effect that could occur with a handover at position A.

VI. Conclusion

A prototype indoor ultrasonic communication network with ceiling-mounted base station transceivers and one mobile transceiver was proposed, constructed and successfully imple-

mented to show proof of concept. The communication cells were hexagonal to cover the service area more efficiently. The separation of different base stations was set at 0.6 m according to the experimental maximum lateral displacement for data transmissions with no measurable errors. An asynchronous positioning method was implemented to determine the location of the mobile transceiver. The ranging signals were phase modulated by different 31-bit Gold codes from the same family using a non-communication channel at 25 kHz. The achieved ranging accuracy was within 28.37 mm with a maximum update rate of 32.3 Hz. The system executed the handover of the communication link on a switch on and off basis as all base stations used the same frequency bands between 45 kHz and 65 kHz for data transmission. Within a circular range of 0.15 m, 16QAM-OFDM was used to achieve a higher uplink data transfer rate of 37.4 kb/s while the range was extended up to 0.35 m by using QPSK-OFDM with a data rate of 18.7 kb/s. For the uplink connection, the achieved data rates using 16QAM-OFDM and QPSK-OFDM were 36.1 kb/s and 18.1 kb/s, respectively. A more robust handover technique using received signal strength with hysteresis was also proposed to improve the system efficiency when multiple mobile devices used the service.

References

[1] M. Kumagai, T. Ura, Y. Kuroda, and R. Walker, "A new autonomous underwater vehicle designed for lake environment monitoring," *Adv. Robot.*, vol. 16, no. 1, pp. 17–26, 2002.

[2] H. Ochi, Y. Watanabe, and T. Shimura, "Basic study of underwater acoustic communication using 32-quadrature amplitude modulation," *Jpn. J. Appl. Phys.*, vol. 44, no. 6S, pp. 4689 – 4693, 2005.

[3] H. Ochi and T. Fukuchi, "Development of tilted toroidal beam wideband transducer using quadrature phase shift keying for underwater acoustic communication," *Jpn. J. Appl. Phys.*, vol. 46, no. 7S, pp. 4961 – 4967, 2007.

[4] T.-H. Won and S.-J. Park, "Design and implementation of an omni-directional underwater acoustic micro-modem based on a low-power micro-controller unit," *Sensors*, vol. 12, no. 2, pp. 2309–2323, 2012.

[5] W. Jiang and W. M. D. Wright, "Progress in airborne ultrasonic data communications for indoor applications," in *Proc. IEEE Int. Conf. Industrial Informatics (INDIN)*, Jul. 2016, pp. 322–327.

[6] R. Adler, P. Desmares, and J. Spracklen, "An ultrasonic remote control for home receivers," *IEEE Trans. Consum. Electron.*, vol. CE-28, no. 1, pp. 123–128, Feb. 1982.

[7] S. Holm, O. Hovind, S. Rostad, and R. Holm, "Indoors data communications using airborne ultrasound," in *Proc. IEEE Int. Acoust. Speech. Signal (ICASSP)*, vol. 3, 2005, pp. 957–960.

[8] M. Hazas and A. Hopper, "Broadband ultrasonic location systems for improved indoor positioning," *IEEE Trans. Mobile Comput.*, vol. 5, no. 5, pp. 536–547, May 2006.

[9] C. Li, D. Hutchins, and R. Green, "Short-range ultrasonic digital communications in air," *IEEE Trans. Ultrason., Ferroelectr., Freq. Control*, vol. 55, no. 4, pp. 908–918, 2008.

[10] W. Jiang and W. M. D. Wright, "Indoor airborne ultrasonic wireless communication using OFDM methods," *IEEE Trans. Ultrason., Ferroelectr., Freq. Control*, vol. 64, no. 9, pp. 1345–1353, 9 2017.

[11] C. F. Chiasserini and R. R. Rao, "Coexistence mechanisms for interference mitigation in the 2.4-GHz ISM band," *IEEE Trans. Wirel. Commun.*, vol. 2, no. 5, pp. 964–975, 9 2003.

[12] W. Guo, W. M. Healy, and M. Zhou, "Impacts of 2.4-GHz ISM band interference on IEEE 802.15.4 wireless sensor network reliability in buildings," *IEEE Trans. Instrum. Meas.*, vol. 61, no. 9, pp. 2533–2544, Sept 2012.

[13] M. Addlesee, R. Curwen, S. Hodges, J. Newman, P. Steggles, A. Ward, and A. Hopper, "Implementing a sentient computing system," *Computer*, vol. 34, no. 8, pp. 50–56, Aug. 2001.

[14] A. Marco, R. Casas, J. Falco, H. Gracia, J. Artigas, and A. Roy, "Location-based services for elderly and disabled people," *Computer Communications*, vol. 31, no. 6, pp. 1055 – 1066, 2008.

[15] C. Medina, J. C. Segura, and . de la Torre, "A synchronous tdma ultrasonic tof measurement system for low-power wireless sensor networks," *IEEE Trans. Instrum. Meas.*, vol. 62, no. 3, pp. 599–611, Mar. 2013.

[16] SensComp, Inc., [Online]. Available: http://www.senscomp.com/pdfs/series-600-environmental-grade-sensor.pdf, accessed Aug. 2015.

[17] S. Jones, *The Basics of Telecommunications*, ser. Basics Books Series. Chicago, IL, USA: International Engineering Consortium, 2004.

[18] A. Jäger, D. Großkurth, M. Rutsch, A. Unger, R. Golinske, H. Wang, S. Dixon, K. Hofmann, and M. Kupnik, "Air-coupled 40-KHz ultrasonic 2D-phased array based on a 3D-printed waveguide structure," in *Proc. IEEE Int. Ultrason. Symp. (IUS)*, Sept. 2017, pp. 1–4.

[19] N. B. Priyantha, A. Chakraborty, and H. Balakrishnan, "The cricket location-support system," in *Proc. 6th Annu. Int. Conf. Mobile Comput. Netw. (MobiCom)*, Aug. 2000, pp. 32–43.

[20] N. B. Priyantha, A. K. Miu, H. Balakrishnan, and S. Teller, "The cricket compass for context-aware mobile applications," in *Proc. 7th Annu. Int. Conf. Mobile Comput. Netw. (MobiCom)*, Jul. 2001, pp. 1–14.

[21] C. Randell and H. Muller, "Low cost indoor positioning system," in *Proc. Ubiquitous Computing*, Sept. 2001, pp. 42–48.

[22] M. M. Saad, C. J. Bleakley, T. Ballal, and S. Dobson, "High-accuracy reference-free ultrasonic location estimation," *IEEE Trans. Instrum. Meas.*, vol. 61, no. 6, pp. 1561–1570, Jun. 2012.

[23] D. Ruiz, E. García, J. Ureña, D. de Diego, D. Gualda, and J. C. García, "Extensive utrasonic local positioning system for navigating with mobile robots," in *Proc. 10th Workshop Positioning Navigat. Commun. (WPNC)*, Mar. 2013, pp. 1–6.

[24] R. J. Milliken and C. J. Zoller, "Principle of operation of NAVSTAR and system characteristics," *Navigation*, vol. 25, no. 2, pp. 95–106, 1978.

[25] B. W. Parkinson and S. W. Gilbert, "NAVSTAR: Global positioning system - Ten years later," *Proc. IEEE*, vol. 71, no. 10, pp. 1177–1186, Oct. 1983.

[26] E. McCune, *Practical digital wireless signals*. Cambridge, U.K.: Cambridge University Press, 2010.

[27] A. Bensky, *Wireless Positioning Technologies and Applications, Second Edition*. Norwood, MA, USA: Artech House, 2016.

[28] R. Gold, "Optimal binary sequences for spread spectrum multiplexing," *IEEE Trans. Inf. Theory*, vol. 13, no. 4, pp. 619–621, Oct. 1967.

[29] R. Pickholtz, D. Schilling, and L. Milstein, "Theory of spread-spectrum communications - a tutorial," *IEEE Trans. Commun.*, vol. 30, no. 5, pp. 855–884, May 1982.

[30] K. Lakhtaria, *Next Generation Wireless Network Security and Privacy*, ser. Advances in Information Security, Privacy, and Ethics. Hershey, PA, USA: IGI Global, 2015.

[31] C. Sertatil, M. A. Altinkaya, and K. Raoof, "A novel acoustic indoor localization system employing CDMA," *Digit. Signal Process.*, vol. 22, no. 3, pp. 506 – 517, 2012.

[32] G. P. Pollini, "Trends in handover design," *IEEE Commun. Mag.*, vol. 34, no. 3, pp. 82–90, Mar. 1996.

[33] V. Vij, *Wireless Communication*. New Delhi, India: Laxmi Publications Pvt Limited, 2010.